International Journal of Civil Engineering

Structure-Concrete

Study on the flexural behaviors of RC beams after freeze-thaw cycles

D. F. CAO[1], W. J. GE[1,2,*], B. Y. WANG[1], Y. M Tu[2,3]

Received: December 2013, Revised: January 2014, Accepted: January 2014

Abstract

In order to investigate the flexural behaviors of RC beams after freeze-thaw cycles, compressive strength test of concrete cubes after 0, 50, 100, 125 freeze-thaw cycles were made, and static flexural experiment of 48 RC beams after 0, 50, 100, 125 freeze-thaw cycles were made. The relationships of relative compressive strength, mass loss rate, relative dynamic elastic modulus and numbers of freeze-thaw cycles were analyzed. The influences of different numbers of freeze-thaw cycles on the flexural behaviors of RC beams with different concrete grades were studied. The results show that concrete cubes' mass, relative dynamic elastic modulus and compressive strength decrease with the increasing of freeze-thaw cycles, and high-strength grade concrete could slow down the damage caused by freeze-thaw cycles. Experimental values of test beams stiffness under short-term load were smaller than theory value. Some under-reinforced RC beams occurs over-reinforced failure mode after freeze-thaw cycles. Boundary reinforcement ratio of RC beams after certain numbers of freeze-thaw cycles was derived and its correctness was verified by experiment. Current code for design of concrete structures about crack load and ultimate load are still suitable for RC beams after freeze-thaw cycles.

Keywords: *Freeze-thaw cycles, Concrete beams, Flexural behaviors, Experimental study.*

1. Introduction

Due to various reasons, concrete structures will fail advance in service process and couldn't reach intended design life, most of which is due to inadequate structural durability. Most China is in the cold zone, especially northeast, there is a partial or large area of destruction due to freeze-thaw cycles. Most existing researches are about the basic mechanical properties of the concrete after freeze-thaw cycles. Alan Richardson [1], Shashank Bishnoi [2], Yanchun Yun [3], Chetan Hazaree [4], J. T. Kevern [5] and other researchers studied the effects of freeze-thaw cycles on ordinary concrete, fiber reinforced concrete, recycled concrete, lightweight sintered pulverized coal ash aggregate concrete, lightweight fly ash aggregate concrete. Song [6], Rami H. Haddad [7], Pierluigi Colombi [8], Shehab M. Soliman [9], Yanchun Yun [10] and other researchers studied the bond behaviors of steel, fiber and concrete subjected to freeze-thaw cycles. Researches about the mechanical behaviors of RC components after freeze-thaw cycles are relative small.

Zhu [11] made experimental study of static flexural behaviors of 16 concrete beams and prestressed concrete beams with three different prestress degrees after freeze-thaw cycles.

Wang [12] made numerical simulation analysis on simply supported beam after 0, 100, 200, 300 freeze-thaw cycles. Zhao [13] studied mechanical behaviors of concrete beams reinforced by GFRP after freeze-thaw cycles. Miao [14] studied mechanical behaviors of concrete beams reinforced by BFRP after freeze-thaw cycles. Ye [15] studied fatigue behaviors of concrete beams reinforced by CFRP after freeze-thaw cycles. Chen [16] made experimental study on the mechanical behaviors of concrete beams reinforced by BFRP after freeze-thaw cycles. Diao [17] studied flexural and shear behaviors of RC beams bearing different sustained load under the action of freeze-thaw cycles and mixed erosion solution. Study the mechanical behavior of concrete structures after freeze-thaw cycles, not only provide basis scientific evaluation on the durability and remaining life prediction of existing building structures ,but also provide technical durability design reference to new projects. This paper focuses on the flexural behaviors of reinforced concrete beams after freeze-thaw cycles.

2. Experiment

2.1. Specimen design

48 reinforced concrete beams for static flexural test

** Corresponding author: gewj@yzu.edu.cn*
1 College of Civil Science and Engineering, Yangzhou University, Yangzhou 225127, China
2 Key Laboratory of Concrete and Prestressed Concrete Structure of Ministry of Education, Southeast University, Nanjing 210096, China
3 Division of Structural Engineering, Luleå University of Technology, SE-971 87, Luleå, Sweden

[Downloaded from ijce.iust.ac.ir on 2026-09-06]

[DOI: 10.22068/IJCE.13.1.92]

were made; cross-section dimensions and reinforcement details of test beam are shown in Fig. 1. Where width *b*=100mm, height *h*=150mm, length *l*=1000mm, length *a*=300mm, length *m*=300mm, length *s*=50mm, concrete cover thickness *c*=20mm. HRB335 grade steel bars were used as tensile and erection reinforcement, diameter of 4mm cold-drawn wire was used ad stirrup. C40, C50 grade concrete were adopted. Design freeze-thaw cycles were 0, 50, 100, 125 times [18]. Specimen parameters are shown in Table 1. Mechanical properties of steel bars are shown in Table 2.

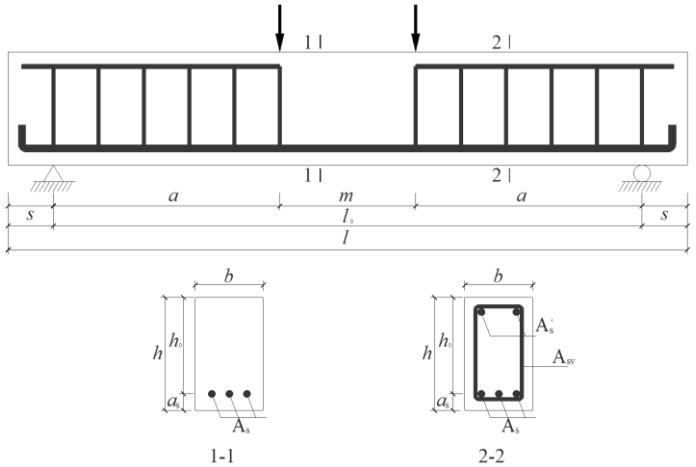

Fig.1 Reinforcements of specimens

Table 1 Parameters of specimens

NO.	*m*	f_c'	A_s	A_s'	A_{sv}	*n*
LA1	3	C40	2Φ10	2Φ8	Φ4@50	0
LA2	3	C40	2Φ10	2Φ8	Φ4@50	50
LA3	3	C40	2Φ10	2Φ8	Φ4@50	100
LA4	3	C40	2Φ10	2Φ8	Φ4@50	125
LB1	3	C40	2Φ12	2Φ8	Φ4@50	0
LB2	3	C40	2Φ12	2Φ8	Φ4@50	50
LB3	3	C40	2Φ12	2Φ8	Φ4@50	100
LB4	3	C40	2Φ12	2Φ8	Φ4@50	125
LC1	3	C50	2Φ12	2Φ8	Φ4@50	0
LC2	3	C50	2Φ12	2Φ8	Φ4@50	50
LC3	3	C50	2Φ12	2Φ8	Φ4@50	100
LC4	3	C50	2Φ12	2Φ8	Φ4@50	125
LD1	3	C50	2Φ14	2Φ8	Φ4@50	0
LD2	3	C50	2Φ14	2Φ8	Φ4@50	50
LD3	3	C50	2Φ14	2Φ8	Φ4@50	100
LD4	3	C50	2Φ14	2Φ8	Φ4@50	125

Note: *m*, number of members; *n*, numbers of freeze-thaw cycles; f_c', concrete grade; A_s, longitudinal tensile reinforcement; A_s', erection reinforcement; A_{sv}, stirrups.

Table 2 Mechanical property of steel bars

Specifications	f_y /N·mm^{-2}	f_u/N·mm^{-2}	E_s/N·mm^{-2}
Φ10	372.7	526.2	2.0×10^5
Φ12	489.1	632.3	2.0×10^5
Φ14	402.2	525.5	2.0×10^5
Φ4	502.5	613.2	2.0×10^5

Note: f_y, yield stress; f_u, ultimate stress; E_s, elastic modulus.

Test concrete mixture ratio was shown in Table 3. Ordinary Portland cement strength grade 42.5 produced by Yangzhou Yadong cement Co. was used, and its 28 days average compressive strength was 52.0MPa; Fine aggregate river sand from Jiangxi Ganjiang was used, and its continuous gradation fineness modulus is 2.6, clay

[Downloaded from ijce.iust.ac.ir on 2026-09-06]

[DOI: 10.22068/IJCE.13.1.92]

content is 0.5%, mud content is 0.2%; Coarse aggregate gravel from Nanjing Luhe was used, and its continuous gradation is 5~31.5mm, clay content is 0.8%; Fly ash of class II from Yizheng Huasheng was used; Water reducing agent SBTJM-9 of 18%water-reducing rate produced by Jiangsu Sobute new Materials Co., Ltd. was used as admixture. Ratio of water to cementitious material of C40, C50 is 0.40, 0.36, litter than maximum ratio of water to cementitious material 0.55, meet the requirement of current code for design of concrete structures. Tested slump of C40 and C50 are all 140mm.

Table 3 Concrete mixture ratio (units kg/m^3)

Grade	water	cement	sand	gravel	fly ash	admixture
C40	173	380	712	1103	50	6.02
C50	173	436	666	1123	45	7.22

2.2. Freeze-thaw cycles test

A group of three 400mm×100mm×100mm prism specimens of C40, C50 were made to measure the mass and relative dynamic elastic modulus loss of specimen after freeze-thaw cycles. Five groups of three 100mm×100mm×100mm test cubes were made to measure the change of concrete compressive strength of specimen after freeze-thaw cycles. Rapid water freeze-thaw cycles method was adopted, minimum and maximum temperatures of the specimen centers should be controlled at (-17±2) ℃ and (6±2) ℃, every freeze-thaw cycle control in about 3 hours. After corresponding freeze-thaw cycles, take out prism specimens, observing external damage, measure the mass and horizontal frequency of the specimen. When reached design number of freeze-thaw cycles, compressive strength test were made. Horizontal frequency test was shown in figure 2.

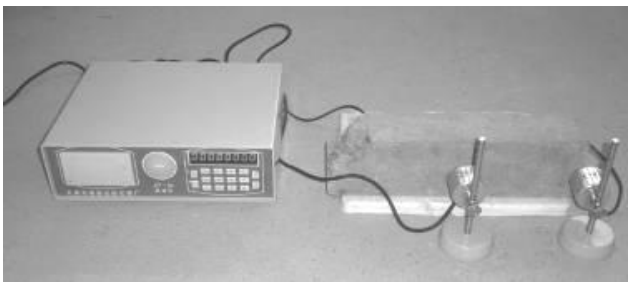

Fig. 2 Horizontal frequency test

2.3. Static flexural test

Components were loaded on 5000kN reaction frame in structure laboratory of Yangzhou University. Design beam is simply supported beam, one end is holder support, and another end is rolling bearing support. In order to prevent concrete local crushing, steel plates were embedded in support and loading point. The hydraulic jack pressure distribution through the distribution beams, and loading values were measured by pressure sensor. Actual loading device is shown in Fig. 3.

Fig. 3 Experimental set-up

Measurement of reinforcement strain: Two strain gauges were arranged in the mid-span of each component's reinforcement. BE120-2AA-type strain gauge produced by Shanxi Zhongyuan measuring instrument factory were used, the resistance value is 120.0 ± 0.1, and sensitivity coefficient is 2.05±1%. Glue 502 was used to paste strain gauge on the surface of polished smooth steel bars, gauze dipped epoxy was used to package train gauge to protection against the tide.

Measurement of concrete strain: according to the design of experiment, installation dial indicator on both sides of the component to measure concrete tension and compression strain, and in order to facility measure the concrete crack width of reinforcement height, one of the dial indicator which originally located in tension zone was moved to the bottom of the component.

Measurement of maximum deflection of component: in order to get the change rules of deflection vary with loading, glass was pasted on the mid-span of components' bottom, and dial indicator was installed to measure the displacement of test beam mid-span. Both ends of the beam were also installed dial indicator to eliminate the influence of supports settlement to the deformation of mid-span.

Measurement of crack width: Brush both sides of the beam on the surface of a layer with diluted lime, and draw 50mm × 50 mm square grids after dry. Observed cracks and accurate measure crack width with crack observation instrument (crack observation instrument accuracy is 0.02mm), and measure the crack length (precision is 0.5mm) with a ruler. Draw cracks extension and development after each load stage on the recording paper, and finally cracks was shot with a digital camera.

Collection of test data: during the test, the strain gage data is automatically collected by static strain TS3890 programmable processing instrument systems produced by Yangzhou Taishi Electronics Co., Ltd.,. Component deformations were measure by dial indicator fixed on the test point. Manual recording was used to observe the crack development and crack width. The value of dials, steel strain, cracks trends, crack width were all measured until the reading stable.

3. Analysis on the Freeze-Thaw Test

3.1. Flaking form

Flaking form of test beams after 0, 50, 100, 125 freeze-

[Downloaded from ijce.iust.ac.ir on 2026-09-06]

[DOI: 10.22068/IJCE.13.1.92]

thaw cycles are shown in Fig. 4. As can be seen from the figure, the surface laitance of concrete beams surface layer slightly peeling after 50 freeze-thaw cycles. the surface mortar peeling and corners missing phenomenon occurs and a small amount of coarse aggregate exposed after 100 freeze-thaw cycles. a lot of coarse aggregate exposed and edges missing serious while freeze-thaw cycle up to 125 times. Compared flaking form of the two grade concrete specimens, it could be found that flaking degree of C50 grade concrete was lower than the C40 under the same freeze-thaw cycles.

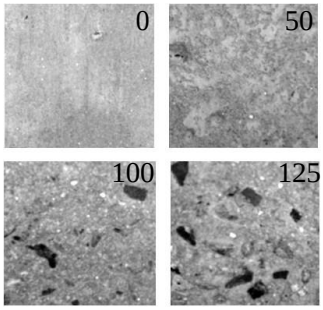

Fig. 4 Surface spalling of beams after freeze-thaw cycles

3.2. Mass loss rate

The mass loss rate of prism specimens after different number of freeze-thaw cycles are shown in Fig. 5. As can be seen from the figure, concrete mass is not reduced when the freeze-thaw cycles less than 25 times, a slight increase on the contrary, preliminary analysis is no spalling concrete situation due to less freeze-thaw cycles, and specimen internal porosity increases after freeze-thaw cycles lead to water content increases. Concrete quality begins decrease while freeze-thaw cycles over 50 times. Mass loss reached 5% while freeze-thaw cycles over 125 times, it is indicate that the concrete have been damaged after 125 freeze-thaw cycles. Specimens C50 mass loss rate is lower than C40 with the same numbers of freeze-thaw cycles, so high strength concrete can slow the destruction of freeze-thaw cycles.

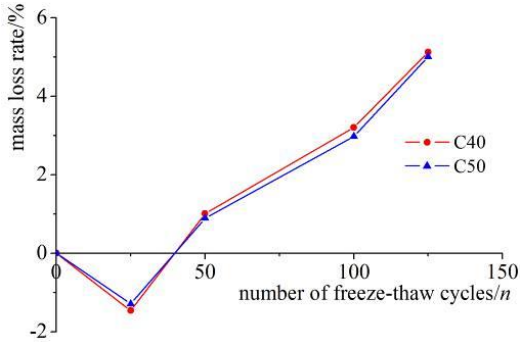

Fig. 5 Curves of mass loss rate and number of freeze-thaw cycles

3.3. Relative dynamic elastic modulus

The relative dynamic elastic modulus of prism specimens after different number of freeze-thaw cycles are shown in Fig. 6. As can be seen from the figure, Concrete relative dynamic elastic modulus decreased with the increasing of freeze-thaw cycles, so concrete internal damage increases with the increasing of freeze-thaw cycles. C40 concrete relative dynamic elastic modulus is lower than C50 concrete with the same number of freeze-thaw cycles.

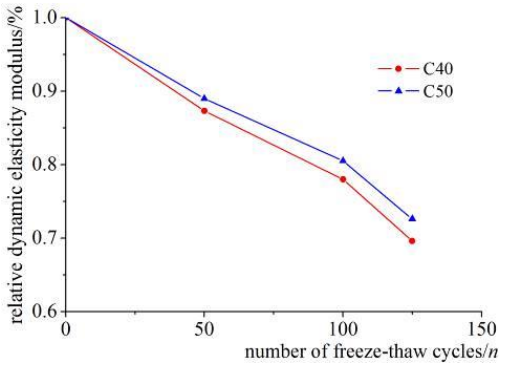

Fig. 6 Curves of relative dynamic elasticity modulus and number of freeze-thaw cycles

Elastic modulus of concrete after freeze-thaw cycles could calculate as E_0^D/E_0=0.9832-0.0076n. Where E_0^D, elastic module of concrete after freeze-thaw cycles; E_0, initial elastic modulus of concrete; n, numbers of freeze-thaw cycles. Elastic module of concrete C40 and C50 after freeze-thaw cycles were listed in Table 4.

Table 4 Concrete elastic module and strength standard value after freeze-thaw cycles

Concrete grade	n	E_0^D/GPa	f_{cu}/N·mm^{-2}	f_{tk}/N·mm^{-2}
C40	0	32.50	45.80	2.85
	50	19.60	39.63	2.63
	100	7.25	32.09	2.40
	125	1.08	24.91	2.04
C50	0	34.50	51.50	2.94
	50	20.81	44.79	2.72
	100	7.70	36.62	2.44
	125	1.15	29.96	2.18

Note: E_0^D, elastic module of concrete after freeze-thaw cycles; n, numbers of freeze-thaw cycles; f_{cu}, concrete axial compression strength standard value after freeze-thaw cycles; f_{tk}, concrete axial tensile strength standard value after freeze-thaw cycles.

3.4. Compressive strength analysis

Concrete cube compressive strength were test after certain numbers of freeze-thaw cycles, and it was listed in Table 4. Define the ratio of concrete compressive strength after freeze-thaw cycles $f_{cu,m}$ to the strength before freeze-thaw cycles $f_{cu,m}^0$ as relative compressive strength $f_{cu,m}/f_{cu,m}^0$, the relationship curve of relative compressive strength and freeze-thaw cycles are shown in Fig. 7.

As can be seen from Fig. 7, concrete cube compressive strength decreases with the increasing of freeze-thaw cycles. Two grades concrete strength decrease laws were similar, concrete compressive strength dropped to about

[Downloaded from ijce.iust.ac.ir on 2026-09-06]

[DOI: 10.22068/IJCE.13.1.92]

86% when the number of freeze-thaw cycles up to 50 times. Concrete compressive strength decreased rapidly to about 72% when numbers of freeze-thaw cycles up to 100 times. Concrete compressive strength dropped to 55% when numbers of freeze-thaw cycles up to 125 times. Concrete compressive strength decreased to about 31% when numbers of freeze-thaw cycles up to 150 times. C40 relative compressive strength of concrete is lower than C50 concrete with the same numbers of freeze-thaw cycles.

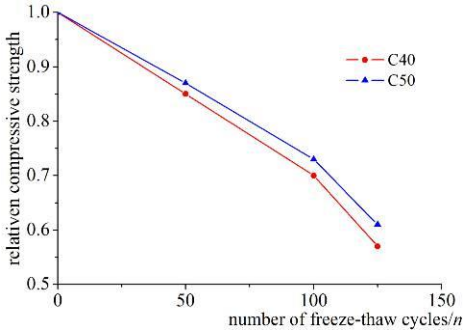

Fig. 7 Curves of relative compressive strength and number of freeze-thaw cycles

Other researchers of national natural science foundation of China (50978224) have given the relationship of the relative compressive strength and freeze-thaw cycles as follows.

$$f_{d,c}/f_c = a + b \times n \quad (1)$$

Where f_c, compressive strength of concrete cubes under normal condition; $f_{d,c}$, concrete cube compressive strength after different numbers of freeze-thaw cycles; n, numbers of freeze-thaw cycles; a, b, regression coefficient, $a=0.9981-1.4\times10^{-4}f_c$, $b=-0.00916+1.31\times10^{-4}f_c$.

Comparison of fitting curve and experimental data was shown in Fig. 8. As can be seen from Fig. 8, experimental data are in good agreement with theoretical fitting curve. The figure shows that compressive strength decreases with the increasing of freeze-thaw cycles and the compressive strength of high-strength concrete C50 downward lower than concrete C40.

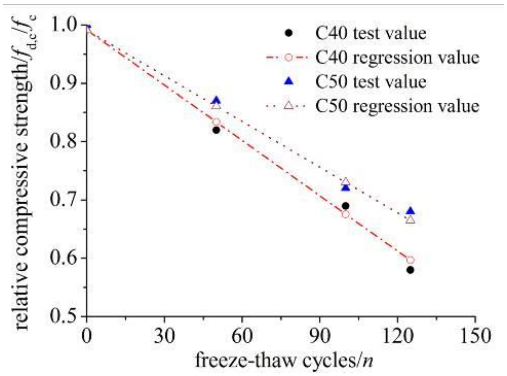

Fig. 8 Comparison of fitting curve and experimental measured data

4. Analysis on the Static Flexural Experiment

4.1. Fracture distribution and failure modes

Some specimen failure mode are shown Fig. 9. Cracks distribution and damage mode of LB4, LD3 and LD4 are similar. Beams occurs elastic deformation in initial loading stage, then first batch vertical cracks occur in pure flexural segment or near loading point. With the increasing of load, crack occurs gradually in flexural segment. With the loads further increase, longitudinal cracks occur in concrete compressive zone, tensile steel bars hasn't yield, over reinforced failure mode occur while balanced failure mode was design with no freeze-thaw cycles. Preliminary analysis is that compressive strength decrease after freeze-thaw cycles, and designed beams' reinforcement ratio were relatively high, so under-reinforced failure mode turn into over-reinforced failure mode after freeze-thaw cycles.

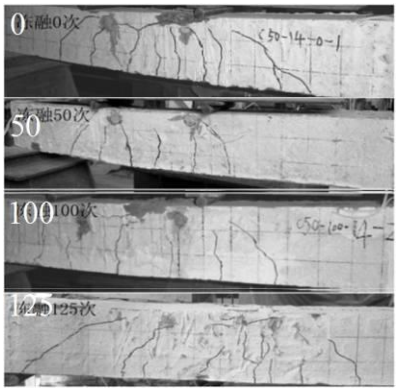

Fig. 9 Distribution of cracks of specimens

Other beams crack distribution and failure modes were similar to under-reinforced beams. Beams occurs elastic deformation in initial loading stage, then first batch vertical cracks occur in pure flexural segment or near loading point. With the increasing of load, cracks occur gradually in flexural segment. With the loads further increase, tensile steel bars yielded and then compressive zone concrete crushed, under-reinforced failure mode occur.

4.2. Freeze-thaw cycles impact on cracking load

Reinforced concrete beams cracking load could calculated according to the code for design of concrete structures [18] as follows:

$$M_{cr} = \gamma W_0 f_{tk} \quad (2)$$

Where W_0, crack resistance moment of translation section; γ, Section resistance plastic impact factor, $\gamma = (0.7+120/h)\gamma_m$, γ_m, basic values of section resistance plastic impact factor, γ_m =1.55, h, height of cross-section, when h>400mm, take h=400mm. f_{tk}, concrete axial tensile strength standard value (experimental values of concrete after freeze-thaw cycles and it was listed in Table 4).

Using measured compressive strength of concrete after freeze-thaw cycles, theoretical cracking load $M_{cr,t}$ of

[Downloaded from ijce.iust.ac.ir on 2026-09-06]

[DOI: 10.22068/IJCE.13.1.92]

reinforced concrete beams calculated according to the current code for design of concrete structures compared with experimental value $M_{cr,e}$ are shown in Table 5, average value of $M_{cr,e}/M_{cr,t}$ is 0.92, variation coefficient is 0.001. As can be seen from the table, theoretical value of cracking load calculate by current code are agree well with experimental value, so crack loading of concrete beams after freeze-thaw cycles could still calculate by China current code for design of concrete structures.

The relationship curves of test beams' cracking load and numbers of freeze-thaw are shown in Fig. 10. As can be seen, cracking load decrease gradually with the increasing of freeze-thaw cycles. The load decline rate of LA, LB beam is slow from 0 to 100 freeze-thaw cycles, and decrease faster after 100 freeze-thaw cycles. As can be seen from the comparison of two grade concrete curves, cracking load of C50 grade concrete beams (LC, LD) decreases rate was lower than C40 grade concrete beams (LA, LB) with the increasing of freeze-thaw cycles.

Table 5 Comparison of theoretical and experimental cracking load, ultimate load

NO.	$M_{cr,t}$/kN·m	$M_{cr,e}$/kN·m	$M_{cr,e}/M_{cr,t}$	$M_{u,t}$/kN·m	$M_{u,e}$/kN·m	$M_{u,e}/M_{u,t}$
LA1	1.76	1.68	0.95	7.02	7.15	1.02
LA2	1.69	1.55	0.92	6.61	6.90	1.04
LA3	1.58	1.42	0.90	6.20	6.64	1.07
LA4	1.36	1.20	0.88	5.70	6.26	1.10
LB1	1.76	1.76	1.00	11.10	11.35	1.02
LB2	1.69	1.57	0.93	10.78	11.08	1.03
LB3	1.58	1.39	0.88	10.26	10.68	1.04
LB4	1.36	1.22	0.89	9.55	10.01	1.05
LC1	1.84	1.77	0.96	11.35	11.52	1.02
LC2	1.73	1.62	0.94	11.00	11.25	1.02
LC3	1.61	1.47	0.91	10.59	10.89	1.03
LC4	1.47	1.32	0.90	10.02	10.41	1.04
LD1	1.84	1.73	0.94	12.34	12.57	1.02
LD2	1.73	1.59	0.92	11.98	12.26	1.02
LD3	1.61	1.45	0.90	11.24	11.70	1.04
LD4	1.47	1.30	0.88	10.15	10.90	1.07

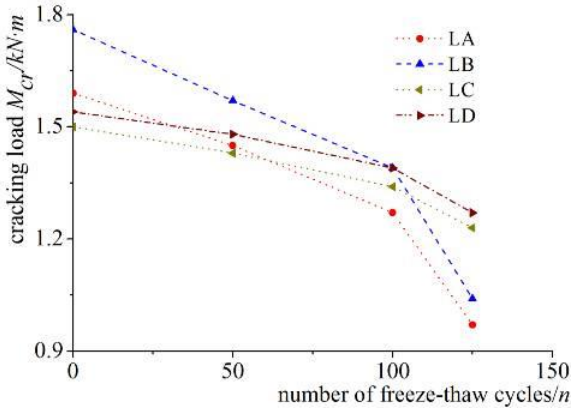

Fig. 10 Curves of cracking load and number of freeze-thaw cycles

4.3. Freeze-thaw cycles impact on ultimate load and ultimate deflection

The relationship curves of ultimate load and freeze-thaw cycles are shown in Fig. 11. Compression strength of concrete and its' bond strength with steel bars decrease due to the increasing of freeze-thaw cycles, then ultimate load of test beams decreased correspondlly. Ultimate load decreased slowly before 100 times freeze-thaw cycles, but decrease faster after 100 times.

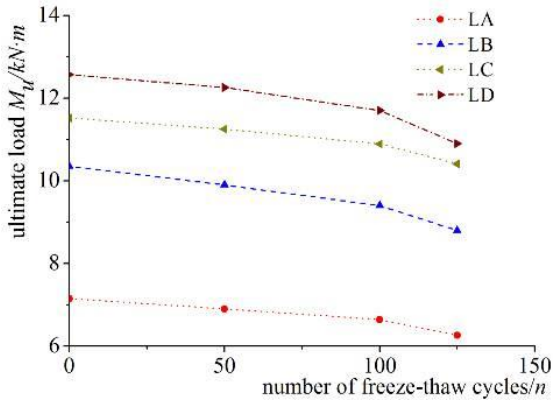

Fig. 11 Curves of ultimate load and number of freeze-thaw cycles

[Downloaded from ijce.iust.ac.ir on 2026-09-06]

[DOI: 10.22068/IJCE.13.1.92]

The relationship curves of load and freeze-thaw cycles are shown in Fig. 12. As can be seen from the figure, components' ultimate capacity decrease with the increasing numbers of freeze-thaw cycles, and ultimate deflection descrease correspondly, indicating that components' ductility decrease with increasing number of freeze-thaw cycles.

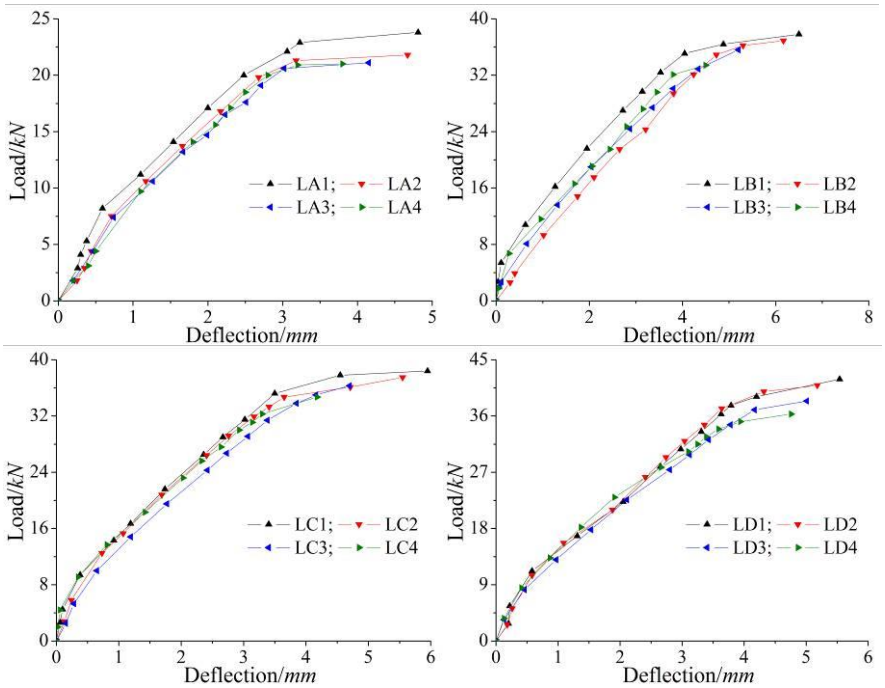

Fig. 12 Relationship curves of load and freeze-thaw cycles

According to average strain plane section assumption, average curvature could calculated as follows.

$$\frac{1}{r}=\frac{M}{B_s}=\frac{\varepsilon_{sm}+\varepsilon_{cm}}{h_0} \tag{3}$$

Where ε_{sm}, average strain of tensile reinforcement; ε_{cm}, average strain of compression concrete; r, average radius of curvature; h_0, effective height of cross-section; B_s, section stiffness under short-term loads.

Cross-section average bending stiffness could be calculated as follows.

$$B_s=\frac{M}{1/r}=M\cdot\frac{h_0}{\varepsilon_{sm}+\varepsilon_{cm}} \tag{4}$$

According to current code for design of concrete structures GB50010-2010, Section stiffness under short-term loads B_s could calculated as follows.

$$B_s=\frac{E_s A_s h_0^2}{1.15\psi+0.2+\frac{6\alpha_E\rho}{1+3.5\gamma_f'}} \tag{5}$$

Where a_E, the elastic modulus ratio of steel bars to concrete, $a_E=E_s/E_c$; ρ, longitudinal tensile reinforcement ratio; ψ, longitudinal reinforcement tensile strain uniformity coefficient between cracks, $\psi=1.1\text{-}0.65f_{tk}/(\rho_{te}\sigma_{sk})$, and $0.2\le\psi\le1.0$. $\rho_{te}=A_s/A_{te}$, longitudinal tensile reinforcement ratio calculated by effective cross-sectional area of tensile concrete, A_{te}, effective cross-sectional area of concrete in tension, for rectangular cross-section flexural members $A_{te}=0.5bh$.

According to formula 5 given by code for design of concrete structures GB50010-2010, stiffness of test beam under short-term load could calculated when consider $M/M_u=0.7$, where M, moment at service stage; M_u, ultimate moment of test beams. Theory stiffness of test beams under short-term load $B_{s,t}$ were compared with experimental stiffness of test beams under short-term load $B_{s,e}$ in Table 6.

As can be seen from Table 6, stiffness of test beam decreases with the increasing of freeze-thaw cycles while concrete grade was the same; stiffness of test beam increase with the increasing of concrete grade or reinforcement ratio while the numbers of freeze-thaw cycles was the same; experimental values of test beams stiffness under short-term load were smaller than theory value, the main reason is freeze-thaw cycles not only reduced elastic modulus of concrete, but also reduced the bond strength between concrete and steel, which resulting in the reducing of the difference of longitudinal steel reinforcement stress, that is, longitudinal reinforcement tensile strain uniformity coefficient between cracks ψ increase, so experimental stiffness of test beam after freeze-thaw cycles reduce larger than theory stiffness which only considered the decreasing of concrete elastic modulus.

[Downloaded from ijce.iust.ac.ir on 2026-09-06]

[DOI: 10.22068/IJCE.13.1.92]

Table 6 Comparison of $B_{s,t}$ and $B_{s,e}$

NO.	$B_{s,e}$ ($10^{10}N\cdot mm^2$)	$B_{s,t}$($10^{10}N\cdot mm^2$)	$B_{s,e}/B_{s,t}$
LA1	28.68	29.69	0.97
LA2	22.84	24.77	0.92
LA3	13.19	14.64	0.90
LA4	2.68	3.13	0.86
LB1	34.62	36.02	0.96
LB2	27.23	29.28	0.93
LB3	14.90	16.32	0.91
LB4	2.82	3.26	0.86
LC1	35.61	36.71	0.97
LC2	28.27	30.01	0.94
LC3	15.44	16.97	0.91
LC4	3.01	3.46	0.87
LD1	41.74	43.25	0.97
LD2	32.15	34.06	0.94
LD3	16.45	17.92	0.92
LD4	2.97	3.40	0.87

4.4. Comparison of theoretical and experimental bearing capacity

Theoretical ultimate load $M_{u,t}$ of reinforced concrete beams calculated according to current code compared with experimental value $M_{u,e}$ are shown in Table 5, average value of $M_{u,e}/M_{u,t}$ is 1.04, variation coefficient is 0.0005. As can be seen from the table, theoretical value of ultimate load calculate by current code are agree well with experimental value, so bearing capacity of concrete beams after freeze-thaw cycles could still calculate by China current code for design of concrete structures.

Bearing capacity calculation diagram of appropriate reinforced RC beams of rectangular cross-section with single reinforcement under freeze-thaw cycles is shown in Fig. 13. Where b, width of cross-section; h, height of cross-section; h_0, effective height of cross-section; x_d, actual height of compression zone; $x_{c,d}$, conversion height of compression zone; A_s, cross-section area of longitudinal tensile steel bars; $\varepsilon_{cu,d}$, concrete ultimate compression strain after freeze-thaw cycles; ε_y, yield strain of steel bars; $M_{u,d}$, ultimate moment of RC beams after freeze-thaw cycles; f_y, yield stress of steel bars; $a_{1,d}$, the ratio of equivalent concrete compressive strength to concrete axial compressive strength.

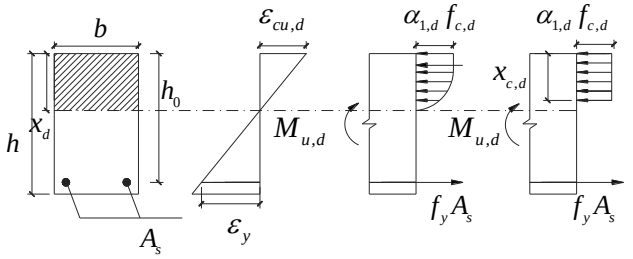

Fig. 13 Calculation diagram

According to the forces and moments balance of cross section, following formula can be obtained.

$$a_{1,d}f_{c,d}bx_d=f_yA_s \quad (6)$$

$$M_{u,d}=a_{1,d}f_{c,d}bx_d(h_0-x_d/2) \quad (7)$$

Ultimate moment of RC beams after freeze-thaw cycles could be calculated by equation (6) and (7).

Balanced failure occurs when concrete crush and tensile steel bars yield occurs simultaneity, take $x_d=x_{d,b}$, following formula could be derived from formula (6).

$$A_s=a_{1,d}f_{c,d}bx_d/f_y \quad (8)$$

Boundary reinforcement ratio $\rho_{sb,d}$ when balanced failure occurs could be obtained by divide both sides of formula (8) by bh_0.

$$\rho_{sb,d}=a_{1,d}\xi_{b,d}f_{c,d}/f_y \quad (9)$$

Where $\xi_{b,d}=\beta_d x_d/h_0=\beta_d\varepsilon_{cu,d}/(\varepsilon_{cu,d}+\varepsilon_y)$.

Boundary reinforcement ratio $\rho_{sb,d}$ of test RC beams after n times freeze-thaw cycles is shown is Fig. 14.

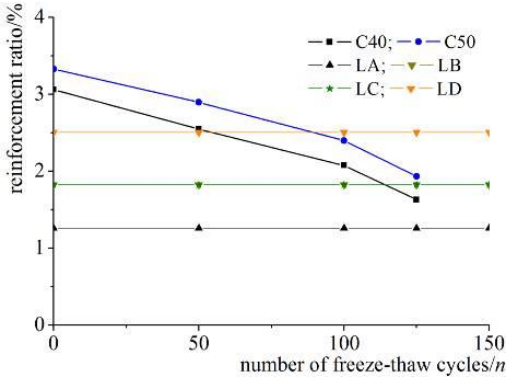

Fig. 14 Curves of boundary reinforcement ratio and number of freeze-thaw cycles

Comparison of boundary reinforcement ratio $\rho_{sb,d}$ of test RC beams after 0, 50, 100, 125 times freeze-thaw cycles and test beams' actual reinforcement ratio are listed in Table 7.

As can be seen from Fig. 14 and Table 7, over-reinforced failure mode occur when actual reinforcement ratio ρ_s of beams LB4, LD3, LD4 larger than the boundary reinforcement ratio $\rho_{sb,d}$, theoretical analysis is in agree with experimental results.

Table 7 Failure pattern discrimination of specimens

NO.	ρ_s/%	n	$\rho_{sd,b}$/%	$\rho_s>\rho_{sd,b}$	Failure mode
LA1	1.26	0	3.06	no	URF
LA2	1.26	50	2.55	no	URF
LA3	1.26	100	2.07	no	URF
LA4	1.26	125	1.63	no	URF
LB1	1.82	0	3.06	no	URF
LB2	1.82	50	2.55	no	URF
LB3	1.82	100	2.07	no	URF

[Downloaded from ijce.iust.ac.ir on 2026-09-06]

[DOI: 10.22068/IJCE.13.1.92]

LB4	1.82	125	1.63	yes	ORF
LC1	1.82	0	3.33	no	URF
LC2	1.82	50	2.90	no	URF
LC3	1.82	100	2.40	no	URF
LC4	1.82	125	1.93	no	URF
LD1	2.50	0	3.33	no	URF
LD2	2.50	50	2.90	no	URF
LD3	2.50	100	2.40	yes	ORF
LD4	2.50	125	1.93	yes	ORF

Note: ρ_s, reinforcement ratio; n, numbers of freeze-thaw cycles; $\rho_{sd,b}$, limits reinforcement ratio; URF, Under-reinforced failure; ORF, over-reinforced failure.

5. Conclusions

Experimental study of concrete cubes, prisms, and rectangular reinforced concrete beams flexural behaviors after freeze-thaw cycles were made, and the conclusions are as follows.

(1) For concrete specimens, surface flake gradually serious with the increasing of freeze-thaw cycles, mass, relative dynamic elastic modulus and cube compressive strength all decrease with the increasing of freeze-thaw cycles;

(2) Cracking load and ultimate load of RC beams decrease with the increasing of freeze-thaw cycles, cracking load of C50 grade concrete beams decreases lower than C40 grade concrete beams with the increasing of freeze-thaw cycles. So high-strength grade concrete could slow down the damage caused by freeze-thaw cycles.

(3) Experimental values of test beams stiffness under short-term load were smaller than theory value which just taking the decreasing of concrete elastic modulus after freeze-thaw cycles into considering, but not consider the decreasing of bond strength between concrete and steel after freeze-thaw cycles.

(4) Some under-reinforced RC beams occurs over-reinforced failure mode after certain numbers of freeze-thaw cycles. Boundary reinforcement ratio of RC beams after freeze-thaw cycles was derived, and its correctness was verified by experiment.

(5) China current code for design of concrete structures about crack load and ultimate load still suitable for RC beams after freeze-thaw cycles, and mechanical properties of concrete parameters after freeze-thaw cycles should be used, boundary reinforcement ratio should be checked when calculate ultimate flexural capacity of RC beams after freeze-thaw cycles.

Acknowledgments: The authors appreciate the support of the national natural science foundation of China (50978224, 51278445, 51308490), natural science foundation for colleges and universities in Jiangsu Province (13KJB560015), the science and technology projects of ministry of housing and urban-rural development (2013-K4-17), the open foundation of Southeast University, Key laboratory of concrete and pre-stressed concrete structure of Ministry of Education, the science and technology projects foundation of Yangzhou City (2012149), the natural science foundation for colleges and universities in Jiangsu Province (13KJB560015).

References

[1] Richardson A, Coventry K. Bacon J. Freeze/thaw durability of concrete with recycled demolition aggregate compared to virgin aggregate concrete, Journal of Cleaner Production, 2011, Vol. 19, pp. 272-277.

[2] Shashank Bishnoi, Taketo Uomoto. Strain-temperature hysteresis in concrete under cyclic freeze-thaw conditions, Cement & Concrete Composites, 2008, Vol. 30, pp. 374-380.

[3] Yanchun Yun, Yu-Fei Wu. Durability of lightweight concretes with lightweight fly ash aggregates, Cold Regions Science and Technology, 2011, Vol. 65, pp. 401-412.

[4] Chetan Hazaree, Halil Ceylan, Kejin Wang. Influences of mixture composition on properties and freeze-thaw resistance of RCC. Construction and Building Materials, 2011, Vol. 25, pp. 313-319.

[5] Kevern JT, Wang K, Schaefer VR. Effect of coarse aggregate on the freeze-thaw durability of pervious concrete, Journal of Materials In Civil Engineering, 2010, Vol. 22, pp. 469-475.

[6] JI Xiaodong, SONG Yupu. Mechanism of bond degradation between concrete and plain steel bar after freezing and thawing, Journal of Building Structures, 2011, No. 1, Vol. 32, pp. 70-74.

[7] Rami H. Haddad, Karim S. Numayr. Effect of alkali-silica reaction and freezing and thawing action on concrete-steel bond, Construction and Building Materials, 2007, Vol. 21, pp. 428-435.

[8] Pierluigi Colombi, Giulia Fava, Carlo Poggi. Bond strength of CFRP-concrete elements under freeze-thaw cycles, Composite Structures, 2010, Vol. 92, pp. 973-983.

[9] Shehab M. Soliman, Ehab El-Salakawy, Brahim Benmokrane. Bond Performance of Near-Surface-Mounted FRP Bars, Composite Structures, 2010, Vol. 92, pp. 973-983.

[10] Yanchun Yun, Yu-Fei Wu. Durability of CFRP-concrete joints under freeze-thaw cycling, Cold Regions Science and Technology, 2011, Vol. 65, pp. 401-412.

[11] Zhu Jiang. Characteristic investigation of the prestressed concrete beams under cycle freezing and thawing. Yangzhou: Master Thesis of Yangzhou University, 2006.

[12] Wang HongWei. Caculation model of reinforced concrete bending members under freeze-thaw environment. Harbin: Master thesis of Harbin Institute of Technology, 2007.

[13] Ren Huitao, Hu Anni, Zhao Guofan. The influence of freeze-thaw action on behavior of concrete beams strengthened by glass fiber reinforced plastics, China Civil Engineering Journal, 2004, No. 4, Vol. 37, pp. 105-110.

[14] MIAO Jijun, ZENG Zaipin, LIU Yanchun, LIU Caiwei, WANG Junfu. Research on behaviors of concrete members strengthened by basalt fiber reinforced plastic sheets under freeze-thaw environment, Journal of Building Structures, 2009, No. s2, pp. 266-269.

[15] Zhang Juanxiu, Ye Jianshu, Yao Weifa. Fatigue behavior of RC beams strengthened with CFRP sheets after freeze-thaw cycling action, Journal of Southeast University (Natural Science Edition), 2010, No. 5, Vol. 40, pp. 1034-1038.

[Downloaded from ijce.iust.ac.ir on 2026-09-06]

[DOI: 10.22068/IJCE.13.1.92]

[16] CHEN Jianwei, HU Haitao, WANG Xibin, CHEN Wei, SUN Yanying. Experiment with the freeze-thaw of the concrete beams reinforced by bfrp, Journal of QingDao Technological University, 2008, No. 3, Vol. 29, pp. 27-30.

[17] DIAO Bo, SUN Yang, MA Bin. Experiment of persistent loading reinforced concrete beams under alternative actions of a mixed aggressive solution and freeze-thaw cycles, Journal of Building Structures, 2009, No. s2, pp. 281-286.

[18] China Academy of Building Research. Code for design of concrete structures GB50010-2010, Beijing, China, Building Industry Press, 2010.

[Downloaded from ijce.iust.ac.ir on 2026-09-06]

[DOI: 10.22068/IJCE.13.1.92]